https://doi.org/10.33263/Materials22.139149

ISSN: 2668-5728 https://materials.international

Materials International

Article

Volume 2, Issue 2, Pages 0139-0149
2020

Received: 04.04.2020
Accepted: 12.04.2020
Published: 14.04.2020

Chitin, Chitosan, and Submicron-Sized Chitosan Particles Prepared from *Scylla serrata* Shells

Nur Alimatul Hakimah Narudin [1], Abdul Hanif Mahadi [2], Eny Kusrini [3], Anwar Usman [2,*]

[1] Department of Chemistry, Faculty of Science, Universiti Brunei Darussalam, Jalan Tungku Link, Gadong BE1410, Brunei Darussalam; 15b3139@ubd.edu.bn
[2] Centre for Advanced Material and Energy Sciences, Universiti Brunei Darussalam, Jalan Tungku Link, Gadong BE1410, Brunei Darussalam; hanif.mahadi@ubd.edu.bn
[3] Department of Chemical Engineering, Faculty of Engineering, Universitas Indonesia, Kampus Baru UI, 16424 Depok, Indonesia; ekusrini@che.ui.ac.id

* Correspondence: anwar.usman@ubd.edu.bn; Scopus ID: 7006491473

Abstract: Extraction of chitin from mud crab (*Scylla serrata*) shells, involving demineralization and deproteinization, and deacetylation of the extracted chitin to form chitosan were investigated. The mud crab chitin and chitosan were obtained with a good yield (16.8% and 84.7% based on dried weight basis). The physicochemical properties, functional groups, molecular weight, and degree of acetylation of the chitin and chitosan were characterized. The surface morphology, the orientation arrangement of polysaccharide strands, and crystallinity of the chitin and chitosan prepared from the mud crab shells were investigated. SEM, FTIR, and XRD analyses demonstrated that the chitin consists of micron-sized fibrils, belonging to α from with the crystallinity of 60.1%. The chitosan has a viscosity-average molecular weight of 6.83 kDa with the degree of acetylation being 9.6% and the crystallinity of 73.8%. The chitosan was successfully fabricated into submicron-sized particles using top-down ionotropic gelation, microwave, and microemulsion methods, employing sodium tripolyphosphate, potassium persulfate, and glutaraldehyde as reagents, respectively. Overall, the results indicated that the preparation of chitin, chitosan, and submicron-sized chitosan particles from mud crab shells could open the opportunity for the value-added seafood waste to be utilized in a wide range of practical applications.

Keywords: Chitin; Chitosan; Chitosan particles; Mud crab; *Scylla Serrata*.

1. Introduction

The rapid global population growth is followed by industries on a massive scale, which requires a large variety of high efficiency materials, therefore exploring new materials to meet the increasing demand is indispensable [1]. Natural biopolymers, including collagen, chitin, silk, alginate, starch, and elastin are among the materials in focus for applications in medical products, cosmetics,

Cite This Article: Narudin, N.A.H.; Mahadi, A.H.; Kusrini, E.; Usman, A. Chitin, chitosan, and submicron-sized chitosan particles prepared from Scylla serrata shells. Mat Int **2020**, 2, 0139-0149.
https://doi.org/10.33263/Materials22.139149

pharmaceuticals, and high-technology industries [2-5]. The biopolymers are of interest due to their low cost of preparation, abundancy, non-toxicity, biocompatibility, biodegradebility, film-forming ability, and low immunogenicity [8-11]. Moreover, the uses of biopolymers which can be extracted from various agricultural waste [12] provide more opportunities to add value to agricultural waste and at the same time to reduce their potential environmental problems.

Most of agricultural waste from seafood industries tend to accumulate due to their low biodegradation rates. Among the seafood waste, the shells of crustaceans such as crabs, lobsters, shrimps, prawns, krill, woodlice, sand hoper, star fish, and barnacles contain 15–40% chitin, which can be isolated by the demineralization and deproteinization. The extracted chitin can be further converted into chitosan by alkaline deacetylation [13]. An additional decolourization step is often applied to remove residual pigments to produce colorless chitin and chitosan [14]. In general, chitin has a predominant chemical structure of poly-β-(1→4)-N-acetyl-D-glucosamine. The deacetylation process removes the acetyl group, leaving the amine group. Based on the arrangement of the polysaccharide strands, chitin and chitosan are divided into α, β, and γ forms, related to alternating antiparallel polysaccharide strands, parallel polysaccharide strands, and two parallel chains alternating with an antiparallel strand, respectively [13]. The different arrangements of the poly-saccharide strands can be distinguished by Fourier transform-infrared (FTIR) spectroscopic and X-ray diffraction (XRD) analyses [13]. Regardless the arrangement of their polysaccharide strands, chitin and chitosan offer many desirable properties, such as having reactive hydroxyl (OH) and amine (NH_2) functional groups useful as chelating agents [15,16]. Both chitin and chitosan show diverse interesting biological properties suitable for many biotechnology, biomedical, pharmaceutical applications [17], and drug carriers [18].

The long biopolymeric chains of chitin and chitosan can be cut into shorter ones using several chemical methods, including coacervation from suspension [19], ionotropic gelation [20], emulsion cross-linking [21], emulsion-droplet coalescence [22], reverse micellar process [23], and sieving [24]. Those methods require surfactants and cross-linking agents, such as Tween-20, glutaraldehyde, and sodium tripolyphosphate (TPP). In contrast, a fascinating microwave method uses strong electrolyte salts [25], such as potassium persulfate and formic acid, without involving any organic solvents, surfactants, or precipitation agents [26-28]. In this case, the size and morphology of the chitosan particles can be controlled by both the concentrations of potassium persulfate and formic acid. The chitosan particles can be complexed with metal ions or organic compounds into composites, enhancing desirable properties for specific applications. For instance, chitosan-lanthanides composites were utilized as adsorbents to remove fluoride ion from drinking water [29], chitin- and chitosan-titania composites were used as an adsorbent/photocatalyst to remove pollutive dyes from water system [30], chitosan-clay composites were applied for packaging materials [31], and chitosan-alginate-fucoidan was successfully developed as a hydrogel wound dressing [32]. In addition, chitosan and hydroxyapatite are the best combinations of biomaterials for the controlling of bone diseases such as osteoporosis and arthritis [33].

The purpose of the present study was to extract chitin from the shells of mud crab (*Scylla serata*), to convert the extracted chitin to chitosan, and to fabricate chitosan particles using three different approaches; namely, emulsion cross-linking, strong electrolyte salts, ionotropic gelation methods. The physicochemical properties, including yield, moisture content, ash content, intrinsic viscosity, molecular weight, degree of acetylation, and surface morphology of chitin, chitosan, and chitosan particles prepared from the mud crab shells were characterized. The vibrational bands of functional groups, crystallinity, and the arrangement of the polysaccharide strands of the chitin and chitosan were evaluated, and the size distribution of the prepared chitosan particles was also determined.

2. Materials and Methods

2.1. Chemicals and sample collection.

All chemicals and reagents, including hydrochloric acid (HCl), formic acid (CH_3COOH), acetic acid (C_2H_5COOH), sodium tripolyphosphate (TPP; $Na_5P_3O_{10}$), sodium hydroxide (NaOH), potassium persulfate ($K_2S_2O_8$), calcium chloride

($CaCl_2$), Tween-20, glutaraldehyde, commercial crab chitosan (CAS No.: 9012-76-4) in analytical grade were purchased from Sigma-Aldrich Co. They were used as received without any further purification. Double distilled water was used all experiments.

Mud crabs (*Scylla serrata*), locally known as *"Ketam kalok"* in Brunei Darussalam, were obtained from local fish market. They were washed thoroughly with water to remove mud, dust, and any other substances that may be present on their outer shells, followed by deshelling to remove their flesh. The shells were then collected and soaked in water to remove any leftover meat, dirt, and impurities. The shells were then sun-dried until their weight was constant. The dried shells were crushed using mortar and pestle and ground into course powder. The approximate powder was then sieved using 355 μm stainless sieve, and the fine particles of mud crab shells were collected.

2.2. Chitin extraction.

In order to isolate chitin, the fine powder of mud crab shells were demineralized using 1 M HCl solution, and the suspension was continuously stirred for 3 hours at room temperature, similar to the isolation procedures of chitin from any crustacean shells [13]. The precipitate was then filtered off under vacuum and rinsed with distilled water until pH value of 7. Then, the demineralized mud crab shells were dried overnight in an oven at 60–70 °C. The demineralized shells powder were deproteinized using 5% NaOH solution with 1:10 w/v ratio. The mixture was stirred and heated at 90–95 °C for 6 hours. The precipitate was filtered under vacuum and washed with distilled water until pH 7 was reached. The resulted chitin was then dried overnight in an oven at 55–60 °C.

2.3. Deacetylation.

The deacetylation of chitin was then conducted according to the method reported by Sarbon et al. (2014) [34]. The dried isolated chitin was treated with 40% NaOH solution with a ratio of chitin to the solution of 1:15 (w/v). The reaction was carried out under stirring at 105 °C for 2 hours. The solution was then filtered off under vacuum and washed with distilled water. The chitosan obtained was then dried for 2 days in an oven at 40 °C.

2.4. Fabrications of chitosan particles.

In this study, three different methods with the same experimental conditions as those reported in literature have been employed to fabricate chitosan particles, as following. First, according to the ionotropic gelation method reported Calvo et al. (1997) [20], the prepared chitosan was dissolved in 1% acetic acid, and the solution was continuously stirred for 8 hours at room temperature, followed by sonication for 40 minutes. Tween-20 (20 mL in water) was then added to the solution. TPP solution (2.5 g L^{-1}) was then added dropwise to the chitosan solution at the ratio of 2:1 (v/v, chitosan to TPP) and particles were spontaneously formed in the solution under mechanical stirring. The suspension was then sonicated for 45 minutes before it was subjected to a membrane filtration followed by oven drying. Second, the chitosan particles were fabricated according to the protocols described previously [27,28]. Here, chitosan (3.00 g) was dissolved in 100 ml of 2% formic acid and the solution was continuously stirred. The pH of the chitosan solution was adjusted to be pH 4. Potassium persulfate (2.0 mmol in water) was added to the solution. The homogenous solution was then subjected to a low power microwave for 5 minutes and it was repeated twice. The mixture was left to cool down at room temperature before drying in an oven to obtain dry chitosan particles. Third, the chitosan particles were fabricated by micro-emulsion method following the protocols described by Maitra et al. (1999) [35]. Chitosan (0.40 g) was dissolved in 60 mL of 0.05 M acetic acid solution at room temperature. 80 mL of 25% glutaraldehyde was then added to the chitosan solution and the mixture was stirred to homogenize. The mixture was then left for 1 hour at room temperature. Tween-20 solution (10 mL in water) was dissolved separately in n-hexane (10 mL) to prepare reverse micelles and it was then added to the mixture containing chitosan and glutaraldehyde under continuous stirring overnight at room temperature. N-hexane was then removed by evaporation at 35 °C using rotary evaporator under low pressure. Excess surfactant was then removed by precipitation with calcium chloride solution. The solution was then subjected to centrifugation at 3000 rpm for 15 minutes. The resulting supernatant containing chitosan particles was filtered off under vacuum and dried in the oven.

2.5. Characterizations.

The yield of the isolated chitin and prepared chitosan was analyzed by comparing their weight before and after the treatment. The surface morphology of the dried powder raw and demineralized mud crab shells along with the extracted chitin and chitosan was assessed using a scanning electron microscopy (SEM) (JSM-7600F, JEOL) operating at 5.0 kV and magnification of 50,000×. Their functional groups and chemical structure were analyzed using a FTIR spectrometer (IR Prestise-21, Shimadzu) in the range of 400–4000 cm^{-1} with 2.0 cm^{-1} spectral resolution, and their crystallinity was determined using X-ray diffraction (XRD-7000, Shimadzu) with Cu Kα radiation (λ = 0.15418 nm) operating at 30 mA and 40 kV. The XRD data were collected over the diffraction 2θ range of 20–80° at a scan rate of 1.0° min^{-1}, respectively.

The size distributions of the chitosan particles were measured using dynamic light scattering (Zetasizer Nano ZS; Malvern Instruments) equipped with a diode-pumped laser (532 nm; 10 mW). The data were fitted with an autocorrelation function and the particle sizes were computed with a non-negative least-squares method.

Physicochemical properties, such as viscosity, molecular weight, moisture content, ash content, the degree of deacetylation of the chitosan of the mud crab shells were analyzed according to the AOAC standard methods, as follows:

2.5.1. Viscosity.

Kinematic viscosity of chitosan (η_c) was determined by Ostwald U-tube viscometer (Cannon Instruments, USA). The measurements were held in acetate buffer in a controlled temperature water bath at 25.0°C. The reference liquid was water (η_r=1.002 cP at 25.0°C), and η_c was calculated using

$$\eta_c = \rho_c \times t \times \eta_r / \rho_r \times t_r \qquad (1)$$

where ρ_c= 1.09398 g mol^{-1} and t is the density and time flow of the chitosan solution, and ρ_r and t_r is the density (0.997 g mol^{-1}) and time flow of water, respectively.

The intrinsic viscosity $[\eta]$, of the prepared chitosan was determined from the linear plot of η_c as a function of the biopolymer concentration in the solution, c, based on the Huggins equation [36];

$$\eta_c = ([\eta] + k[\eta]^2)c \qquad (2)$$

where k is a constant. The $[\eta]$ was estimated by extrapolation to zero concentration. From the $[\eta]$ value, the viscosity-average molecular weight of the prepared chitosan, M, was determined by employing the Mark-Houwink equation [36,37];

$$[\eta] = KM^{\alpha} \qquad (3)$$

where K and α are constants. In the preset study, the measurements were carried out for chitosan dissolved in 0.2 M acetate buffer (pH 4.6), in which K and α constants of chitosan have been reported to be 8.2×10^{-2} and 0.76, respectively [38].

2.5.2. Moisture content.

Dry sample of chitosan was added with water and was then filtered under vacuum. The wet sample of chitosan was weighed (W_1) and dried in an oven until a constant weight was established (W_2). The moisture content was calculated as;

$$\mathit{Moisture}\ \% = (W_1 - W_2)/W_1 \times 100 \qquad (4)$$

2.5.3. Ash Content.

Ash content of the chitosan was determined by combustion of 3.0 g (W_1) of the biopolymer using a constant weight crucible in an oven at 550 °C for 3 hours. After cooling to room temperature, the crucible was kept in a desiccator for 30 minutes, and the ash was weighed (W_2). The ash percentage was calculated as,

$$\mathit{Ash}\ \% = W_2/W_1 \times 100 \qquad (5)$$

2.5.4. Degree of deacetylation.

Degree of deacetylation of the prepared chitosan was determined by acid-base titration according to the procedure reported by Pokhrel et al. (2016) [14]. Here, 0.1 g chitin and chitosan were dissolved in 30 mL of 1 M HCl, and the solution was stirred for 30 minutes at room temperature and titrated against 1 M NaOH solution in the presence of methyl orange indicator. The percent of free NH_2 groups in chitosan was calculated as [39];

$$NH_2\% = (C_1V_1 - C_2V_2) \times 0.016/G \qquad (6)$$

where V_1 and C_1 is the volume and concentration of HCl, C_2 is the concentration of NaOH, V_2 is the volume of NaOH added by titration (mL), and G is the sample weight. Here, the correction on sample weight was neglected, as the chitosan has been dried until its constant weight prior to the experiment. The degree of deacetylation, DA, was then calculated as,

$$DA\ \% = NH_2\ \% / 9.94\% \times 100 \qquad (7)$$

where 9.94 % is the theoretical NH_2 percentage of chitosan.

3. Results and Discussion

3.1. Fabrications of chitosan particles.

The SEM images of the dried powder of raw and demineralized mud crab shells along with the extracted chitin and chitosan are shown in Figure 1. The raw mud crab shells showed the stacking nanofibers with the widths of the fibers being widely distributed over a range from 100 to 200 nm (Figure 1A). Demineralization led the mud crab shell fibers to smaller fibrils which are agglomerated (Figure 1B). Deproteinization made the fibrils into microfibrils stacked on top of each other forming a nonporous, smooth membranous phase consisting cavities and crystalline chitin (Figure 1C). The SEM images also indicated a nonporous, smooth membranous, and flaky chitosan (Figure 1D).

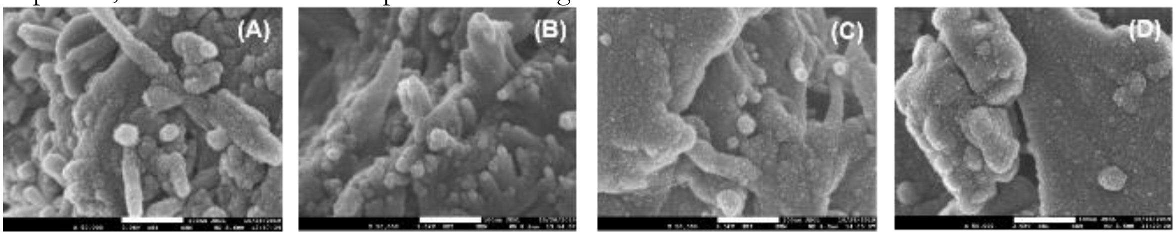

Figure 1. SEM observation of (A) raw shell of mud crab, (B) demineralized shell, (C) chitin, and (D) chitosan. The scale bars denote 500 nm.

3.2. Physicochemical properties.

The extraction yield, moisture content, residual ash content, and other characteristics of the chitin and chitosan prepared from the mud crab shells are also summarized in Table 1. Those extracted from crab and shrimp shells and cuttlefish were also presented for comparison. Ash content of mud crab (*S. serrata*) shells was 37.7%, lower than those of crab and shrimp shells (59.8 and 48.8%, respectively) [40,41], indicating lower mineral contents of the mud crab shells. The extraction yield of chitin was 16.76% with respect to the dried shells. This yield of chitin in this study was higher than that obtained from crab shells (10-27%) but lower than that of the dried shrimp shells (37.4%) [40,41]. This finding suggested that, among the crabs, the mud crab shells is also an important and economical source for chitin [34].

It is noteworthy to recall that deacetylation removes acetyl groups from the polymeric chain of chitin, leaving behind chemically reactive amino group of chitosan [34]. Interestingly, the yield of chitosan upon deaceylation of chitin isolated from mud crab shells was 84.73%, higher than for the deacetylation of chitin isolated from shrimp and crab shells (74.5% and 53.0%, respectively) or mud crab shells reported by Kiruba et al. (53.4%) [42]. This implied that the lower DA of the chitin of mud crab shells (76.4 %) compared those of shrimp (88.5%) and crab shells (78.6%). The deacetylation led to the decrease in DA of chitosan (9.6%), which was lower than the chitosan fabricated from crab shells, comparable with that of shrimp, and lower by a factor of 2 compared with that of cuttlefish. In general, this finding indicated that regardless the source of chitin, the fabricated chitosan contains N-acetyl groups that cannot be completely removed without inducing hydrolysis of the polysaccharide backbone. Therefore, the DA of chitosan depends not only on the source of chitin, but also on deacetylation reaction, concentration of reagents, and prolonged reaction times. The high reactivity of the chitin from mud crab shells against the deacetylation reaction has been ascribed to the trans-arrangement of their acetamido groups in the biopolymeric chains [34]. Since in this study the deacetylation reaction was performed under pseudohomogeneous conditions in the basic solution, the chitin was randomly deacetylated in homogeneous conditions [43]. Thus, the kinetics of such the homogeneous alkaline *N*-deacetylation of chitin should be pseudo-first-order reaction, as previously reported by Sannan et al. (1977) [44].

Table 1. Physicochemical properties, yield, and degree of acetylation of *S. serrata* chitin and chitosan, along with those of crab, shrimp, cuttlefish [41].

	Mud Crab	Crab	Shrimp	Cuttle-fish
Raw material				
Ash (%)	37.7	59.8	48.8	90.6
Moisture (%)	56.3			
Chitin				
Yield	16.8	10	20	5
Ash (%)	2.1	0.5	0.4	0.8
Moisture (%)	9.08			
DA (%)	76.4	78.6	88.5	70.1
Chitosan				
Yield	84.7	53.0	74.5	24.0
Ash (%)	2.0			
Moisture (%)	7.98			
[η] (mL g^{-1})	89	78	175	19
***M* (kDa)**	6.83	6.12	17.03	1.03
DA(%)	9.6	17	12	5 %

Note: The yield was calculated on dried weight basis.

In this study, the moisture content of chitin extracted from the mud crab shells was 9.08% and that of chitosan was 7.98%, which was slightly lower than reported by Kiruba et al. (2013) (9.48%) and much lower than the commercial chitosan (14%)

[42]. The low moisture content of chitosan indicates its stability, good quality, and acceptability for application which limits the moisture of chitosan to be less than 15% [45]. The residual ash content of chitin and chitosan was measured to be in the range of 2.0-2.1%, higher than other that of chitin from snow crab and shrimp (1.07–1.33) [46], but lower than other reported chitin and chitosan from mud crab (5.97%) [42]. The residual ash content might affects the solubility and viscosity of chitin and chitosan. The relatively high residual ash contents indicated that the less effective demineralization of the mud crab shells, due most likely to the low HCl concentration used in this study.

The linear regression of η_c as a function of the chitosan concentration, c, resulted in the intrinsic viscosity $[\eta]$ to be 89 mL g^{-1}, slightly higher than that of chitosan from crab shells (78 mL g^{-1}). By using Eq. (3), with a given set of constants K and α, irrespective of the polydispersity of the sample, the viscosity average M was estimated to be 6.83 kDa, comparable to that of the chitosan prepared from crab shells (6.12 kDa), higher than that of cuttlefish (1.03 kDa), but it was lower than from shrimp shells (17.03 kDa).

3.3. Physicochemical properties.

The chemical structure and functional groups of chitin and chitosan fabricated from mud crab shells have been analyzed using FTIR spectroscopy.

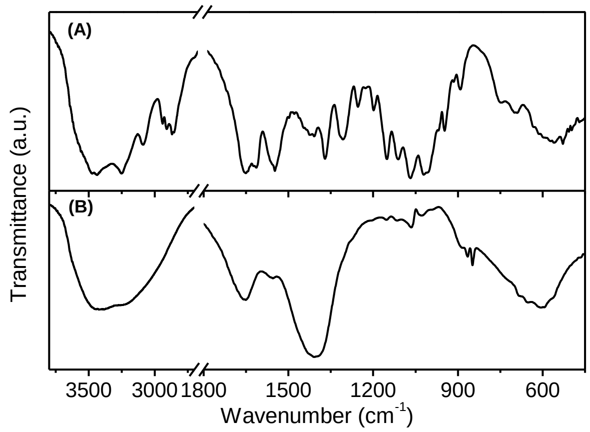

Figure 2. FTIR spectrum of *S. serrata* chitin (A) and chitosan (B).

Figure 2 shows the FTIR spectra of the chitin and chitosan. As shown in Figure 2A, the FTIR spectrum of chitin showed two separate peaks of the vibration modes of amide I at 1630 and 1662 cm^{-1}, due to intermolecular hydrogen bonds between oxygen atom of carbonyl (C=O) group and hydrogen of amine (NH_2) and hydroxyl (OH) groups, interconnecting the biopolymeric chains [47]. The vibrational band of OH showed the detailed structure with two peaks at 3439 and 3497 cm^{-1}, attributed to the intra- and inter-molecular hydrogen bonds involving the OH group [48].

Overall, the FTIR spectrum indicated that the chitin extracted from mud crab shells was in the α-form, similar to those extracted from crab, shrimp, and cuttlefish [41]. The FTIR spectrum of chitosan showed main bands at 3444 and 3223 cm^{-1}, assigned to the vibrations of OH and NH_2 groups, at 1657 cm^{-1} due to the amide carbonyl group, at 1406 cm^{-1} attributed to the stretching vibration of $-CH_2$ groups, and a broad band at 484–825 cm^{-1} due to the bending vibrations of OH and pyranose groups.

3.4. Polysaccharide strands arrangement.

As shown in Figure 3, the XRD spectrum of the chitin and chitosan in the 2θ range of 20–80° exhibited several diffraction peaks indicating their crystallinity. The XRD spectrum of the chitin (Figure 3A) showed a prominent diffraction peak at 26.5°, which is a marker crystalline reflection of α-form of chitin [49]. This finding again unambiguously supports the notion that the chitin isolated from the mud crab shells was the α-form.

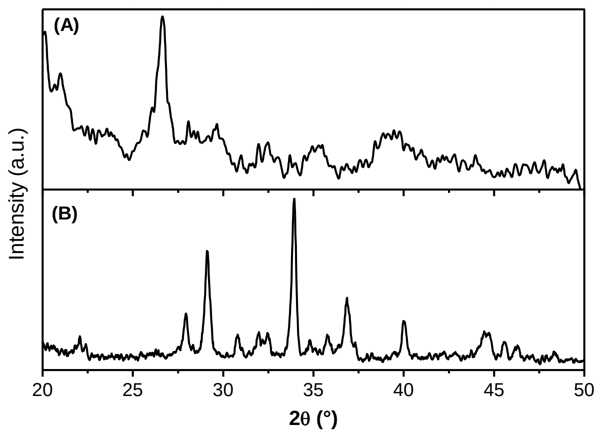

Figure 3. XRD pattern of *S. serrata* chitin (a) and chitosan (b).

Figure 3B shows the diffraction pattern of chitosan with 2θ peaks being at 27.9, 29.2, 33.9, 36.9, 40.0, 44.6, 45.6, and 46.3°. Overall, XRD revealed the crystallinity of the chitin and chitosan extracted from mud crab shells. The relative crystallinity of the biopolymers, which was calculated by dividing the area of the crystalline diffraction peaks with the total area under the curve [50], was estimated to be 60.1% for chitin and was

73.8% for chitosan. As for comparison, the crystallinity of chitin from crab and shrimp shells are in the range of 64.1–67.8%, as the α form chitin tends to have a high crystallinity [51]. Interestingly, the high crystallinity of the chitosan prepared from mud crab shells highlighted its distinct crystalline properties compared with those prepared from crab and shrimp shells (31.9–38.8%) [41].

3.5. Chitosan particles.

The chitosan particles have been fabricated from the mud crab chitosan by three different methods, namely ionotropic gelation, microwave, and microemulsion. It was clearly observed that the chitosan immediately formed cloudy suspension in water, indicating the formation of chitosan particles. This finding indicated that TPP formed the polymeric chains of chitosan into particles, potassium persulfate reacted with the polymeric chains of chitosan and cut them into shorter chains, and glutaraldehyde made microemulsion of chitosan.

Figure 4 shows SEM images of the dried chitosan particles fabricated by three different top-down fabrication methods, suggesting that they were in the form of small-sized spherical particles, agglomerated forming brittle flakes. The SEM images also indicated the high efficiency of the three fabrication methods, which rapidly formed a large number of chitosan particles. The size distributions of the chitosan particles were measured to be in the range of 413–1527 nm with the main peaks being 824, 560, and 471 nm for chitosan particles fabricated by ionotropic gelation, microwave, and microemulsion, respectively. This finding revealed that the top-down methods have successfully fabricated submicron-sized chitosan particles.

In principle, the sizes of chitosan particles prepared from mud crab shells could be dependent on the preparation method, reaction time, and reagent and its concentration to cut the chitosan polymeric chains and to form gel or reverse micellar, which would be resolved in future. Nevertheless, it is noteworthy that, in general, the formation of chitosan particles should be initiated on the surface of chitosan polymer, as it has been pointed out by Kamat et al. (2016) [52]. The short polymer chains were then converted to spherical particles, and the particles grew rapidly into sizeable particles. Finally, particles were agglomerated in the solution resulting in a broad size distribution. The addition of surfactant such as Tween-20 in the microemulsion method could prevent the agglomeration, resulting in smaller particle sizes. With the sizes in the submicron scale, regardless the preparation method and reagent, the chitosan particles prepared from mud crab shells could be potentially utilized for drug carriers and biomedical applications. The complexation of the submicron-sized chitosan particles into composites is also of our current interest.

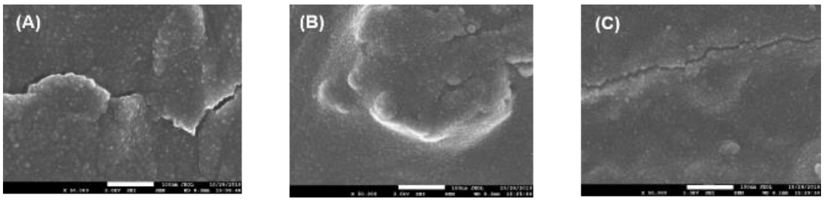

Figure 4. SEM observation of chitosan particles fabricated by (A) ionotropic gelation, (B) microwave, and (C) microemulsion. The scale bars denote 500 nm.

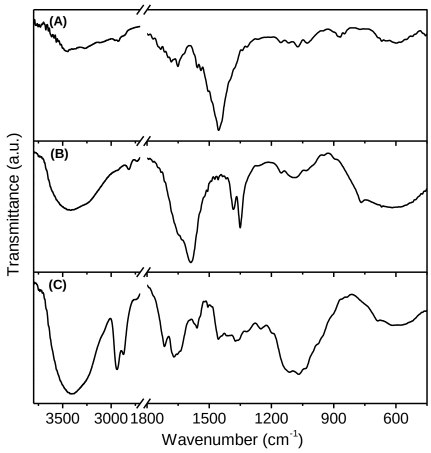

Figure 5. FTIR spectrum of chitosan particles fabricated by (A) ionotropic gelation, (B) microwave, and (C) microemulsion.

FTIR spectrum of chitosan particles fabricated by the three top-down fabrication methods is shown in Figure 5. It is clearly observed that the FTIR spectrum of chitosan particles fabricated by different methods did not resemble each other. It offered an interpretation that the mechanism of the formation of chitosan particles was different, depending on the chemical reactions between the chitosan polymeric chains with the reagent. Thus, the functional groups of the chitosan polymeric chains in the particles have been modified to some extent.

Regardless of the difference in intensity, most of the vibrational bands of the functional groups of chitosan (Figure 2b) were reproduced by the chitosan particles fabricated using microwave and microemulsion methods, employing potassium persulfate, and glutaraldehyde as reagent (Figure 5B and 5C). This was in contrast to that prepared by the ionotropic gelation using TPP as reagent and Tween-20 as a cross linker (Figure 5A). In the latter case, the FTIR spectrum was dominated by a newly emerged band at 1453 cm^{-1}, which may be originated from the cross linker [53]. Therefore, detail analyses on the chemical structures of mud crab chitosan particles and how they can be complexed with organic compounds or polydentate metal ions are indispensable in the future.

4. Conclusions

In conclusion, chitin has been extracted from the shells of mud crab (*Scylla serrata*) shells. The extraction involving demineralization and deproteinization processes resulted in as high as 16.8% yield with respect to dried shells, revealing that the mud crab shells are an important and economical source for chitin. The FTIR spectroscopy and XRD analysis revealed that the chitin prepared from the mud crab shells belonged to the α form. The deacetylation converted the extracted chitin into chitosan with 84.7% yield. The XRD analysis suggested that the chitin and chitosan prepared from the shells of mud crab have a crystallinity of 60.1% and 73.8%, respectively, and SEM images indicated that they are microfibrils stacked on top of each other. The mud crab chitosan has a viscosity-average molecular weight of 6.83 kDa with a degree of acetylation being 9.6%. The chitosan was successfully fabricated into submicron-sized particles with the peak of size distribution being 471, 560, and 824 nm using microemulsion, microwave, and ionotropic gelation methods, employing glutaraldehyde, potassium persulfate, and sodium tripolyphosphate as reagents, respectively. Overall, the results indicated that the chitin, chitosan, and submicron-sized chitosan particles prepared from the wasted shells of mud crab have good physicochemical properties, demonstrating that they might be very promising candidates for practical applications in the fields of biomedical, tissue engineering, adsorbents, and biosensors.

Funding

This research received no external funding

Acknowledgments

The authors are grateful for the support provided by Faculty of Science, University Brunei Darussalam.

Conflicts of Interest

The authors declare no conflict of interest.

References

1. Ige, O.O.; Umoru, L.E.; Aribo, S. Natural products: A minefield of biomaterials. *ISRN Mater. Sci.* **2012**, *2012*, 1–20, https://doi.org/10.5402/2012/983062.

2. Kennedy, J.F.; Knill, C.J.; Thorley, M. Natural polymers for healing wounds. *Recent Adv. Environ. Compat. Polym.* **2001**, 97–104, https://doi.org/10.1533/9781845693749.2.97.

3. Wu, H.; Li, F.; Wang, S.; Lu, J.; Li, J.; Du, Y.; Sun, X.;

Chen, X.; Gao, J.; Ling, D. Ceria Nanocrystals decorated mesoporous silica nanoparticle based ROS-scavenging tissue adhesive for highly efficient regenerative wound healing. *Biomaterials* **2018**, *151*, 66–77, https://doi.org/10.1016/j.biomaterials.2017.10.018.
4. Gupta, A.; Rattan, V.; Rai, S. Efficacy of chitosan in promoting wound healing in extraction socket: A prospective study. *J. Oral Biol. Craniofac. Res.* **2019**, *9*, 91–95, https://doi.org/10.1016/j.jobcr.2018.11.001.
5. Gohil, S.V.; Suhail, S.; Rose, J.; Vella, T.; Nair, L.S. Polymers and composites for orthopedic applications. In: *Materials for Bone Disorder*. Bose, S.; Bandyopadhyay, A. Eds.; Academic Press: London, UK, 2007; pp. 349–403, https://doi.org/10.1016/B978-0-12-802792-9.00008-2.
6. Yadav, P.; Yadav, H.; Shah, V. G.; Shah, G.; Dhaka, G. Biomedical biopolymers, their origin and evolution in biomedical sciences: A systematic review. *J. Clin. Diagn. Res.* **2015**, *9,* 21–25, https://doi.org/10.7860/JCDR/2015/13907.6565.
7. Celli, A.; Sabaa, M.W.; Jyothi, A.N.; Kalia, S. Chitosan and starch-based hydrogels via graft copolymerization. In: *Polymeric Hydrogels as Smart Biomaterials Springer Series on Polymer and Composite Materials*. Kalia, S. Ed.; Springer: Cham, Switzerland, 2015; pp. 189–234, https://doi.org/10.1007/978-3-319-25322-0_8.
8. Kumar, M.N.V.R.; Muzzarelli, R.A.A.; Muzzarelli, C.; Sashiwa, H.; Domb, A.J. Chitosan chemistry and pharmaceutical perspectives. *Chem. Rev.* **2004**, *104,* 6017–6084, https://doi.org/10.1021/cr030441b.
9. Younes, I.; Rinaudo, M. Chitin and chitosan preparation from marine sources. Structure, properties and applications. *Mar. Drugs* **2015**, 1133–1174, https://doi.org/10.3390/md13031133.
10. Rizeq, B.R.; Younes, N.N.; Rasool, K.; Nasrallah, G. K. Synthesis, bioapplications, and toxicity evaluation of chitosan-based nanoparticles. *Int. J. Mol. Sci.* **2019**, *29*, 5776, https://doi.org/10.3390/ijms20225776.
11. Lee, D.W.; Lim, H.; Chong, H.N.; Shim, W.S. Advances in chitosan material and its hybrid derivatives: A review. *Open Biomater. J.* **2009**, *1*, 10–20, https://doi.org/10.2174/1876502500901010010.
12. Nitta, S.K.; Numata, K. Biopolymer-based nanoparticles for drug/gene delivery and tissue engineering. *Int. J. Mol. Sci.* **2013**, *14*, 1629–1654, https://doi.org/10.3390/ijms14011629.
13. Yadav, M.; Goswami, P.; Paritosh, K.; Kumar, M.; Pareek, N.; Vivekanand, V. Seafood waste: A source for preparation of commercially employable chitin/chitosan materials. *Bioresour. Bioprocess.* **2019**, *6,* https://doi.org/10.1186/s40643-019-0243-y.
14. Pokhrel, S.; Yadav, P.N.; Adhikari, R. Applications of chitin and chitosan in industry and medical science: A review. *Nepal J. Sci. Technol.* **2016**, *16*, 99–104, https://doi.org/10.3126/njst.v16i1.14363.
15. Elsoud, M.M.A.; Kady, E.M.E. Current trends in fungal biosynthesis of chitin and chitosan. *Bull. Nat. Res. Centre* **2019**, *43*, https://doi.org/10.1186/s42269-019-0105-y.
16. Knidri, H.E.; Belaabed, R.; Addaou, A.; Laajeb, A.; Lahsini, A. Extraction, chemical modification and characterization of chitin and chitosan. *Int. J. Biol. Macromol.* **2018**, *120*, 1181–1189, https://doi.org/10.1016/j.ijbiomac.2018.08.139.
17. Dutta, J. Isolation, purification, and nanotechnological applications of chitosan. In: *Polysaccharides: Bioactivity and Biotechnology*. Ramawat, K.; Mèrillon, J.M. Eds.; Springer: Cham, Switzerland, 2015; pp. 1029–1063, https://doi.org/10.1007/978-3-319-16298-0_45.
18. Kusrini, E.; Arbianti, R.; Sofyan, N.; Abdullah, M.A.A.; Andriani, F. Modification of chitosan by using samarium for potential use in drug delivery system. *Spectrochim. Acta A: Mol. Biomol. Spectr.* **2014**, *120*, 77–83, https://doi.org/10.1016/j.saa.2013.09.132.
19. Lengyel, M.; Kállai-Szabó, N.; Antal, V.; Laki, A.J.; Antal, I. Microparticles, microspheres, and microcapsules for advanced drug delivery. *Sci. Pharm.* **2019**, *87*, 1–31, https://doi.org/10.3390/scipharm87030020.
20. Calvo, P.; Remuñan-Lopez, C.; Vila-Jato, J.L.; Alonso, M.J. Novel hydrophilic chitosan-polyethylene oxide nanoparticles as protein carriers. *J. Appl. Polym. Sci.* **1997**, *63*, 125–132, https://doi.org/10.1002/(SICI)1097-4628(19970103)63:1<125::AID-APP13>3.0.CO;2-4.
21. Rieggera, B.R.; Bäurera, B.; Mirzayevaa, A.; Tovar, G.E.M.; Bach, M. A systematic approach of chitosan nanoparticle preparation via emulsion crosslinking as potential adsorbent in wastewater treatment. *Carbohydr. Polym.* **2018**, *180*, 46–54, https://doi.org/10.1016/j.carbpol.2017.10.002.
22. Garg, U.; Chauchan, S.; Jain, N. Current advances in chitosan nanoparticles based drug delivery and targeting. *Adv. Pharm. Bull.* **2019**, *9*, 195–204, https://doi.org/10.15171/apb.2019.023.
23. Zhao, L.M.; Shi, L.E.; Zhang, Z.L.; Chen, J.M.; Shi, D.D.; Yang, J.; Tang, Z.X. Preparation and application of Chitosan Nanoparticles and Nanofibers. *Braz. J. Chem. Eng.* **2011**, *28*, 353–362, https://doi.org/10.1590/S0104-66322011000300001.
24. Agnihotri, S.A.; Mallikarjuna, N.N.; Aminabhavi, T.M. Recent advances on chitosan-based micro- and nanoparticles in drug delivery. *J. Control. Release* **2004**, *100*, 5–28, https://doi.org/10.1016/j.jconrel.2004.08.010.

25. Zaharoff, D.A.; Rogers, C.J.; Hance, K.W.; Schlom, J.; Greiner, J.W. Chitosan solution enhances both humoral and cell-mediated immune responses to subcutaneous vaccination. *Vaccine* **2007**, *25*, 2085–2094, https://doi.org/10.1016/j.vaccine.2006.11.034.

26. Hsu, S.C.; Don, T.M.; Chiu, W.Y. Free radical degradation of chitosan with potassium persulfate. *Polym. Degrad. Stab.* **2002**, *75*, 73–83, https://doi.org/10.1016/S0141-3910(01)00205-1.

27. Kusrini, E.; Shiong, N.S.; Harahap, Y.; Yulizar, Y.; Dianursanti, D.; Arbianti, R.; Pudjiastuti, A.R. Effect of monocarboxylic acids and potassium persulfate on preparation of chitosan nanoparticles. *Int. J. Technol.* **2015**, *6*, 11–21, https://doi.org/10.14716/ijtech.v6i1.778.

28. Usman, A.; Kusrini, E.; Widiantoro, A.B.; Hardiya, E.; Abdullah, N.A.; Yulizar, Y. Fabrication of chitosan nanoparticles containing samarium ion potentially applicable for fluorescence detection and energy transfer. *Int. J. Technol.* **2018**, *9*, 1112–1120, https://doi.org/10.14716/ijtech.v9i6.2576.

29. Kusrini, E.; Paramesti, S.N.; Zulys, A.; Daud, N.Z.A.; Usman, A.; WIlson, L.D.; Sofyan, N. Kinetics, isotherm, thermodynamic and bioperformance of defluoridation of water using praseodymium-modified chitosan. *J. Environ. Chem. Eng.* **2019**, *7*, 1-10, https://doi.org/10.1016/j.jece.2019.103498.

30. Weltrowski, M.; Martel, B.; Morcellet, M. Chitosan N-benzyl sulfonate derivatives as sorbents for removal of metal ions in an acidic medium. *J. Appl. Polym. Sci.* **1996**, *59*, 647–654, https://doi.org/10.1002/(SICI)1097-4628(19960124)59:4<647::AID-APP10>3.0.CO;2-N.

31. Haerudin, H.; Pramono, A.W.; Kusuma, D.S.; Jenie, A.; Voelcker, N.H.; Gibson, C. Preparation and characterization of chitosan/montmorillonite (MMT) nanocomposite systems. *Int. J. Technol.* **2010**, *1*, 65–73.

32. Murakami, K.; Aoki, H.; Nakamura, S.; Nakamura, S.; Takikawa, M.; Hanzawa, M.; Kishimoto, S.; Hattori, H.; Tanaka, Y.; Kiyosawa, T.; Sato, Y.; Ishihara, M. Hydrogel blends of chitin/chitosan, fucoidan and alginate as healing-impaired wound dressings. *Biomaterials* **2010**, *31*, 83–90, https://doi.org/10.1016/j.biomaterials.2009.09.031.

33. Gritsch, L.; Maqbool, M.; Mouriño, V.; Ciraldo, F.E.; Cresswell, M.; Jackson, P.R.; Lovell, C.; Boccaccini, A.R. Chitosan/hydroxyapatite composite bone tissue engineering scaffolds with dual and decoupled therapeutic ion delivery: Copper and strontium. *J. Mater. Chem. B* **2019**, *7*, 6109–6124, https://doi.org/10.1039/c9tb00897g.

34. Sarbon, N.; Sandanamsamy, S.; Kamaruzaman, S.; Ahmad, F. Chitosan extracted from mud crab (scylla olivicea) shells: physicochemical and antioxidant properties. *J. Food Sci. Technol.* **2014**, *52*, 4266-4275, https://doi.org/10.1007/s13197-014-1522-4.

35. Maitra, A.; Kumar Ghosh, P.; De, T.K.; Sahoo, S.K. Process for the preparation of highly monodispersed polymeric hydrophilic nanoparticles. U.S. Patent 5,874,111, February 23, 1999.

36. Lapasin, R.; Pricl, S. Industrial applications of polysaccharides. In: *Rheology of Industrial Polysaccharides: Theory and Applications.* Lapasin, R.; Pricl, S. Eds.; Springer: Boston, MA, USA, 1995; pp. 134–161, https://doi.org/10.1007/978-1-4615-2185-3_2.

37. Brugnerotto, J.; Desbrières, J.; Roberts, G.; Rinaudo, M. Characterization of chitosan by steric exclusion chromatography. *Polymer* **2001**, *42*, 09921–09927, https://doi.org/10.1016/S0032-3861(01)00557-2.

38. Rinaudo, M.; Milas, M.; Dung, P.L. Characterization of chitosan. Influence of ionic strength and degree of acetylation on chain expansion. *Int. J. Biol. Macromol.* **1993**, *15*, 281–285, https://doi.org/10.1016/0141-8130(93)90027-J.

39. Yuan, Y.; Chesnutt, B.M.; Haggard, W.O.; Bumgardner, J.D. Deacetylation of chitosan: Material characterization and in vitro evaluation via albumin adsorption and pre-osteoblastic cell culture. *Materials* **2011**, *4*, 1399–1416, https://doi.org/10.3390/ma4081399.

40. Tolaimate, A.; Desbrières, J.; Rhazi, M.; Alagui, A.; Vincendon, M.; Vottero, P. On the influence of deacetylation process on the physicochemical characteristics of chitosan from squid chitin. *Polymers* **2000**, *41*, 2463–2469, https://doi.org/10.1016/S0032-3861(99)00400-0.

41. Hajji, S.; Younes, I.; Ghorbel-Bellaaja, O.; Hajji, R.; Rinaudo, M.; Nasri, M.; Jellouli, K. Structural differences between chitin and chitosan extracted fromthree different marine sources. *Int. J. Biol. Macromol.* **2014**, *65*, 298–306, https://doi.org/10.1016/j.ijbiomac.2014.01.045.

42. Kiruba, A.; Uthayakumar, V.; Munirasu, S.; Ramasubramanian, V. Extraction, Characterization and physico chemical properties of chitin and chitosan from mud crab shell (Scylla Serrata). *Indian J. Appl. Res.* **2013**, *3*, 44-46.

43. Kurita, K.; Sannan, T.; Iwakura, Y. Studies on chitin, IV. Evidence for formation of block and random copolymers of N-acetyl-D-glucosamine and D-glucosamine by hetero-and homogeneous hydrolyses. *Die Makromolekulare Chemie* **1977**, *178*, 3197–3202, https://doi.org/10.1002/macp.1977.021781203.

44. Sannan, T.; Kurita, K.; Iwakura, Y. Studies on chitin.

V. Kinetics of deacetylation reaction. *Polym. J.* **1977**, *9*, 649–651, https://doi.org/10.1295/polymj.9.649.
45. Ocloo, F.; Quayson, E.; Adu-Gyamfi, A.; Quarcoo, E.; Asare, D.; Serfor-Armah, Y.; Woode, B. Physicochemical and functional characteristics of radiation-processed shrimp chitosan. *Radiat. Phys. Chem.* **2011**, *80*, 837–841, https://doi.org/10.1016/j.radphyschem.2011.03.005.
46. Kucukgulmez, A.; Celik, M.; Yanar, Y.; Sen, D.; Polat, H.; Kadak, A.E. Physicochemical characterization of chitosan extracted from Metapenaeus stebbingi shells. *Food Chem.* **2011**, *126*, 1144–1148, https://doi.org/10.1016/j.foodchem.2010.11.148.
47. Focher, B.; Naggi, A.; Torri, G.; Cosani, A.; Terbojevich, M. Structural differences between chitin polymorphs and their precipitates from solutions—Evidence from CP-MAS 13C-NMR, FT-IR and FT-Raman spectroscopy. *Carbohydr. Polym.* **1992**, *17*, 97–102, https://doi.org/10.1016/0144-8617(92)90101-U.
48. Pearson, F.G.; Marchessault, R.H.; Liang, C.Y. Infrared spectra of crystalline polysaccharides. V. Chitin. *J. Polym. Sci.* **1960**, *43*, 101–116, https://doi.org/10.1002/pol.1960.1204314109.
49. Cárdenas, G.; Cabrera, G.; Taboada, E.; Miranda, S. P. Chitin characterization by SEM, FTIR, XRD, and ^{13}C cross polarization/mass angle spinning NMR. *J. Appl. Polym. Sci.* **2004**, *93*, 1876–1885, https://doi.org/10.1002/app.20647.
50. Wan, Y.; Creber, K.A.M.; Pebbley, B.; Tam Bui, V. Ionic conductivity and related properties of crosslinked chitosan membranes. *J. Appl. Polym. Sci.* **2003**, *89*, 306–317, https://doi.org/10.1002/app.12090.
51. Abdou, E.S.; Nagy, K.S.; Elsabee, M.Z. Extraction and characterization of chitin and chitosan from local sources. *Bioresour. Technol.* **2008**, *99*, 1359–1367, https://doi.org/10.1016/j.biortech.2007.01.051.
52. Kamat, V.; Bodas, D.; Paknikar, K. Chitosan nanoparticles synthesis caught in action using microdroplet reactions. *Sci. Rep.* **2016**, *6*, 1–4, https://doi.org/10.1038/srep22260.
53. Nazeera Banu, V.R.; Rajendran, S.; Senthil Kumaran, S. Investigation of the inhibitive effect of Tween 20 self assembling nanofilms on corrosion of carbon steel. *J. Alloys Compd.* **2016**, *675*, 139–148, https://doi.org/10.1016/j.jallcom.2016.02.247.